Biochem. J. (2013) **454**, 275–282 (Printed in Great Britain) doi:10.1042/BJ20130046

online data

A general anaesthetic propofol inhibits aquaporin-4 in the presence of Zn^{2+}

Jungo KATO*†, Mariko Kato HAYASHI†, Shinnosuke AIZU†, Yoshinori YUKUTAKE‡, Junzo TAKEDA* and Masato YASUI†[1]

*Department of Anesthesiology, School of Medicine, Keio University, Tokyo 160-8582, Japan, †Department of Pharmacology, School of Medicine, Keio University, Tokyo 160-8582, Japan, and ‡Department of Biochemistry, School of Medicine, Keio University, Tokyo 160-8582, Japan

AQP4 (aquaporin-4), a water channel protein that is predominantly expressed in astrocyte end-feet, plays an important role in the brain oedema formation, and is thereby considered to be a potential therapeutic target. Using a stopped-flow analysis, we showed that propofol (2,6-diisopropylphenol), a general anaesthetic drug, profoundly inhibited the osmotic water permeability of AQP4 proteoliposomes in the presence of Zn^{2+}. This propofol inhibition was not observed in AQP1, suggesting the specificity for AQP4. In addition, the inhibitory effects of propofol could be reversed by the removal of Zn^{2+}. Other lipid membrane fluidizers also similarly inhibited AQP4, suggesting that the modulation of protein–lipid interactions plays an essential role in the propofol-induced inhibition of AQP4. Accordingly, we used Blue native PAGE and showed that the profound inhibition caused by propofol in the presence of Zn^{2+} is coupled with the reversible clustering of AQP4 tetramers. Site-directed mutagenesis identified that Cys^{253}, located at the membrane interface connecting to the C-terminal tail, is responsible for Zn^{2+}-mediated propofol inhibition. Overall, we discovered that propofol specifically and reversibly inhibits AQP4 through the interaction between Zn^{2+} and Cys^{253}. The findings provide new insight into the functional regulation of AQP4 and may facilitate the identification of novel AQP4-specific inhibitors.

Key words: aquaporin 4 (AQP4), brain oedema, general anaesthetic, water channel.

INTRODUCTION

Brain oedema remains a major cause of morbidity and mortality following diverse pathological conditions such as stroke, brain tumours, meningitis or systemic diseases [1,2]. In particular, in cytotoxic brain oedema, an abnormal uptake of water by neurons and glia during the early phase of brain injury is suggested to play an important role in the activation of a number of signalling cascades that further exacerbate brain damage [2–4]. Despite the pathophysiological relevance of brain oedema, no established prophylactic treatment exists at present.

The swelling of pericapillary astrocyte end-feet is an early finding in cytotoxic brain oedema formation [5]. Since AQP4 (aquaporin-4), a water-specific channel, is strongly localized in pericapillary astrocyte end-feet [6], AQP4 has been hypothesized to play an essential role in cytotoxic brain oedema [7–9]. Indeed, *AQP4*$^{-/-}$ mice show reduced brain water accumulation and an improved outcome under several pathological conditions [10,11]. Therefore the elucidation of the underlying mechanisms responsible for the functional regulation of AQP4 and the identification of AQP4 modulators is of utmost importance.

We have shown previously that the water permeability of AQP4 can be inhibited by heavy metal ions such as Zn^{2+}, Cu^{2+} and Hg^{2+} in experiments using AQP4 proteoliposomes [12,13]. Since the intracellular concentration of Zn^{2+} in astrocytes can increase up to several hundred micromolars under pathological conditions such as oxidative stress or hyperosmotic stress [14], the effects of Zn^{2+} on AQP4 are of especially great interest, although the weak inhibitory effects of Zn^{2+} may not be sufficient to serve as a clinically applicable AQP4 inhibitor. Alternatively, the pharmacological modulation of the inhibitory effects of Zn^{2+} could be an interesting target for the development of a novel AQP4 inhibitor.

Propofol (or 2,6-diisopropylphenol) is a lipophilic intravenous anaesthetic drug that is used extensively for the induction and maintenance of general anaesthesia. Although the underlying pharmacological mechanisms responsible for its anaesthetic action remain elusive, propofol is generally accepted to affect the function of pLGICs (pentameric ligand-gated ion channels) such as inhibitory $GABA_A$ (γ-aminobutyric acid type A) receptors and excitatory nicotinic acetylcholine receptors by binding specifically to proteins [15]. On the other hand, propofol is also known to influence the functions of diverse types of structurally unrelated membrane proteins [16], probably by modulating protein–lipid interactions through its effects on the lipid membrane environment [17,18]. Interestingly, several studies have shown that propofol attenuates brain oedema in cerebral ischaemic injury animal models [19,20]. Thus whether propofol can alter the function of AQP4 is a point of interest.

In the present study, we used a proteoliposome functional assay to demonstrate that propofol can reversibly and specifically inhibit the water permeability of AQP4 in the presence of Zn^{2+}. A biochemical analysis using BN-PAGE (Blue native PAGE) also revealed that the profound inhibition caused by the combination of propofol and Zn^{2+} is coupled with the clustering formation of multiple AQP4 tetramers. These studies provide a novel framework to elucidate further the regulation of AQP4 and may facilitate the identification of new AQP4 inhibitors.

EXPERIMENTAL

Drugs and chemicals

Propofol, ascorbyl palmitate, α-tocopherol, capsaicin and phenetyl alcohol (all purchased from Wako Pure Chemical Industries) were freshly dissolved in DMSO (Wako Pure

Abbreviations used: AQP, aquaporin; BN-PAGE, Blue native PAGE; $GABA_A$, γ-aminobutyric acid type A; hAQP, human AQP; NMM, *N*-methylmaleimide; OAP, orthogonal arrays of particle; P_f, osmotic water permeability; pLGIC, pentameric ligand-gated ion channel.

[1] To whom correspondence should be addressed (email myasui@a3.keio.jp).

Chemical Industries) just before use. The final concentration of DMSO applied to liposomes was less than 0.2 %, which was shown to have little effect on the water permeability of AQP proteoliposomes. EDTA was purchased from Sigma–Aldrich. Other materials are described in detail below.

Expression and purification of His-tagged AQPs

cDNAs encoding His_6-tagged hAQP4 (human AQP4) (M1 isoform and M23 isoform) were subcloned into baculovirus expression vector pTripleEX-4 (Novagen) and transfected into Sf9 insect cells with Bacvector 1000 DNA (Novagen) to obtain baculovirus particles. The AQP4 C178S, C253S and C178S/C253S double mutant proteins were obtained using QuikChange II Site Directed Mutagenesis kit (Agilent Technologies). All constructs were fully confirmed by sequencing. Expression of the wild-type and mutant AQP4 protein in Sf9 insect cells was carried out as reported previously [21]. cDNA encoding His_{10}-tagged hAQP1 was subcloned into yeast expression vector pYES2 (Invitrogen) and expression of hAQP1 was performed in yeast culture as described previously [13]. Purification of the proteins was performed by nickel affinity chromatography as described previously [13,21].

Reconstitution of purified AQPs into liposomes

Purified AQPs were reconstituted into liposomes by a dilution method as described previously [13]. A reconstitution mixture was prepared by combining 100 mM Mops (pH 7.5), 15 mg/ml *n*-octyl β-D-glucopyranoside (Dojindo Laboratories), 17.5 mg/ml sonicated lipids, 20 mM carboxyfluorescein and 100 μg/ml purified AQP protein. The lipid composition was *Escherichia coli* total lipid extract (chloroform/ether preparation; Avanti Polar Lipids) and the saturated fatty acid mixture at a mass ratio of 2.5:1. The saturated fatty acid mixture was composed of DPPC (dipalmitoyl phosphatidylcholine; NOF), cholesterol and 1,5-dihexadecyl-*N*-succinyl-L-glutamate (Nippon Fine Chemical) at a molar mixture of 5:5:1. The mixture was injected into 25 vol. of assay buffer (100 mM Mops, pH 7.5) to dilute the detergent. Liposomes were harvested by ultracentrifugation [45 min at 50 000 rev./min (rotor type 50.1 Ti; Beckman Coulter) at 4 °C] and resuspended in assay buffer for three cycles to remove the residual detergent. The diameter of the proteoliposomes was measured with the dynamic light-scattering method using N4 Sub-Micron Particle Analyzer (Beckman Coulter).

Measurement of the osmotic water permeability of proteoliposomes

The P_f (osmotic water permeability) of AQP4 proteoliposomes was measured by a carboxyfluorescein quenching method [22], using a stopped-flow apparatus with a dead time of <3 ms (Unisoku). AQP4 proteoliposomes (100 μl) were rapidly mixed with the same volume of hyperosmotic solution (100 mM Mops, pH 7.5, and 400 mM sucrose) at 22 °C. The λ_{ex} was 491.5 nm (measured with a monochrometer), and the λ_{em} was >515 nm (measured with a cut-on filter). Averaged data from multiple determinations were fitted to double exponential curves with the aid of IGOR Pro 5.03J software (WaveMetrics). The fitting parameters were then used to determine the P_f by first applying the linear conversion from relative fluorescence into relative volume and then iteratively solving the P_f equation:

$$P_f = [dV(t)/dt]/[(SAV)(MVW)(C_{in} - C_{out})]$$

where $V(t)$ is the relative intra-vesicular volume as a function of time, SAV is the vesicular surface area to volume ratio, MVW is the molar volume of water (18 cm^3/mol), and C_{in} and C_{out} are the initial concentrations of total solute inside and outside the vesicle respectively. The apparent artificial enhancement of fluorescence intensity caused by lipophilic compounds in liposome solutions were subtracted from the raw data before the analyses.

BN-PAGE and immunoblotting

BN-PAGE for proteoliposomes was performed as described previously with small modifications [23]. Proteoliposomes were lysed with NativePAGE™ Sample Buffer (Invitrogen) containing 1 % dodecyl-β-D-maltoside (Invitrogen) for 30 min on ice. Lysates were centrifuged at 15 000 rev./min for 30 min at 4 °C, and the pellets were discarded. Total protein content was determined by Bradford assay. The protein (1–5 μg) was mixed with Coomassie Brilliant Blue G-250 at a detergent:dye ratio of 4:1, loaded on to a BN-PAGE (4–16 % Bis-Tris gel) along with NativeMARK molecular mass markers, and run with NativePAGE running buffers according to the manufacturer's protocol (Invitrogen). The proteins were transferred to a PVDF membrane, and then incubated with rabbit anti-(hAQP4 IgG) antibody (Sigma–Aldrich). The membrane was probed with HRP (horseradish peroxidase)-conjugated anti-(rabbit IgG) antibody (GE Healthcare Bio-Sciences). Immunoreactive bands were visualized by ECL® chemiluminescence detection system (GE Healthcare Bio-Sciences).

Sucrose-density-gradient fractionation

AQP4 proteoliposomes were lysed with 1 % *n*-dodecyl-β-D-maltoside (Invitrogen) for 30 min on ice and separated by ultracentrifugation [16 h at 200 000 ***g*** (rotor type SW 60 Ti; Beckman Coulter) at 4 °C] on a linear sucrose density gradient (up to 40 % sucrose in 100 mM Mops buffer, containing 0.05 % *n*-dodecyl-β-D-maltoside) prepared by a linear gradient mixer (Advantec MFS). Each fraction was collected in a 0.5 ml volume from the top of the gradient using an automatic fraction collector (Advantec MFS) and analysed by immunoblotting for AQP4.

RESULTS

Propofol profoundly and specifically inhibits the P_f of AQP4 proteoliposomes in the presence of Zn^{2+}

Although the putative targets of propofol for its anaesthetic action are believed to be pLGICs such as inhibitory $GABA_A$ receptors and excitatory nicotinic acetylcholine receptors, propofol is also known to modify the functions of diverse types of membrane proteins [15,16]. Since propofol also attenuates brain oedema after brain injury [19,20], we first examined whether propofol altered the water permeability of AQP4 in a proteoliposome functional assay system using purified AQP4 protein (M23 isoform). However, the P_f of AQP4 proteoliposomes was not remarkably altered by the single application of propofol [$P_f = 53.4 \pm 17.0$ μm/s (mean $\pm$ S.D.) ($n = 9$) compared with $P_f = 53.7 \pm 19.0$ μm/s ($n = 12$) for a DMSO-treated group; $P = 1$] (Figure 1C).

As reported previously, the P_f of AQP4 can be dynamically regulated in a Zn^{2+}-dependent manner [13]. Thus we next investigated whether propofol can modulate the function of AQP4 in the presence of Zn^{2+}. In agreement with the previous study, the P_f of the AQP4 proteoliposomes was weakly inhibited in the presence of Zn^{2+} [$P_f = 38.7 \pm 16.0$ μm/s,

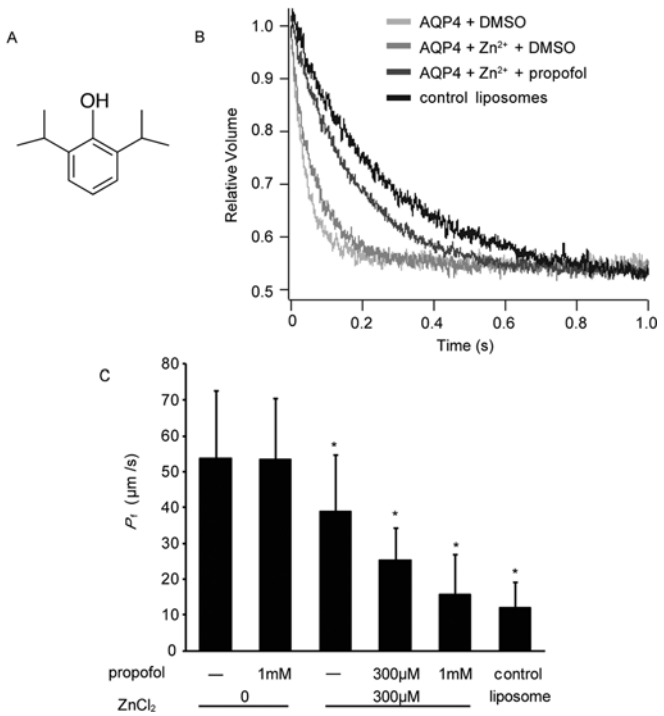

Figure 1 Propofol inhibits the P_f of AQP4 proteoliposomes in the presence of Zn^{2+}

(**A**) A chemical structure of propofol. (**B**) Representative time courses for the hyperosmotic shrinkage of AQP4 proteoliposomes incubated with 0.1 % DMSO; 300 μM $ZnCl_2$ for 5 min, followed by 0.1 % DMSO for 15 min; or 300 μM $ZnCl_2$ for 5 min, followed by 1 mM propofol for 15 min as indicated; results for control liposomes without AQP4 are also shown (black). Treatments were performed at room temperature (22 °C), and the stopped-flow measurements were performed at 22 °C. (**C**) P_f of AQP4 proteoliposomes treated with $ZnCl_2$ and propofol. AQP4 proteoliposomes were treated as indicated and the P_f values were calculated from the relative volume changes measured using the stopped-flow apparatus. The P_f of control liposomes is displayed as a negative control. The results are shown as the means $\pm$ S.D. ($n = 5$–12). $^*P < 0.05$, compared with no-treatment group as analysed using a Student's unpaired t test.

28 ± 11.8 % inhibition ($n = 12$); $P<0.05$]. Surprisingly, propofol profoundly inhibited the P_f of AQP4 in the presence of Zn^{2+} [$P_f = 15.7 \pm 11.1$ μm/s (treated with 1 mM propofol and 300 μM $ZnCl_2$), 69.9 ± 14.7 % inhibition ($n = 8$)] (Figures 1B and 1C). To rule out the possibility of non-specific effects caused by the His-tag in the AQP4 proteins used for purification, we also examined the effects of propofol and Zn^{2+} on AQP4 proteoliposomes without the His-tag; similar results were obtained (Supplementary Figure S1 at http://www.biochemj.org/bj/454/bj4540275add.htm). Moreover, the inhibitory effects of propofol in the presence of Zn^{2+} were also observed in AQP4 M1 proteoliposomes, which is the other splicing isoform that has a longer N-terminus than AQP4 M23 (Supplementary Figure S2 at http://www.biochemj.org/bj/454/bj4540275add.htm).

Additionally, to determine whether propofol inhibits other AQPs, we examined the effects of propofol on AQP1 proteoliposomes, which is structurally the most similar water channel to AQP4 among the AQP family. As reported previously [13], an inhibitory effect of Zn^{2+} alone was not observed for AQP1 proteoliposomes [$P_f = 87.3 \pm 12.6$ μm/s compared with $P_f = 89.8 \pm 25.9$ μm/s in DMSO-treated group ($n = 4$) respectively; $P = 1$] (Figure 2). Furthermore, the combined effects of propofol and $ZnCl_2$ on the P_f of AQP1 proteoliposomes were not as apparent as those on AQP4 proteoliposomes [$P_f = 77.4 \pm 8.7$ μm/s ($n = 4$)]. These findings indicate that propofol specifically inhibits the water permeability of AQP4.

Lipid membrane fluidization has a key role in propofol inhibition

Although some observations suggest that specific drug–protein interactions are essential for the propofol-induced functional modification of ion channels, a non-specific perturbation of the lipid bilayer by propofol has also been proposed to explain its pharmacological diversity. Propofol modifies the physiological properties of the lipid membrane through antioxidizing effects [24,25] or lipid membrane fluidizing effects [18]. Thus we hypothesized that the alteration of the lipid membrane environment may play a crucial role in the propofol-induced inhibition of AQP4. To test this possibility, we examined whether other lipophilic antioxidants (ascorbyl palmitate and α-tocopherol) or lipid membrane fluidizers (capsaicin and phenethyl alcohol) might have similar effects on AQP4 proteoliposomes. As shown in Figure 3, however, neither of the lipophilic antioxidants showed any remarkable inhibition of AQP4 even in the presence of Zn^{2+}. On the other hand, all the tested lipid membrane fluidizers showed a significant inhibition of the P_f of AQP4 proteoliposomes in the presence of Zn^{2+}, as observed with propofol. These findings suggest that lipid membrane fluidization has an essential role in propofol-induced inhibition.

Propofol facilitates Zn^{2+}-mediated clustering of AQP4 proteins on the lipid membrane

To elucidate the underlying mechanisms by which propofol-induced lipid membrane fluidization affected AQP4 function, we subsequently performed a BN-PAGE analysis. As described in previous papers [26,27], BN-PAGE is ideally suited for visualizing protein–protein interactions within the lipid membrane, enabling us to determine whether the combination of Zn^{2+} and propofol can promote the lateral rearrangement and assembly of AQP4 proteins through tetramer–tetramer interactions, which may lead to functional alteration. As shown in Figure 4(A), AQP4 proteins were mainly detected as single or double tetramers in AQP4 proteoliposomes without treatment. The treatment with Zn^{2+} alone did not show any band shifts, whereas propofol alone showed a slight tendency towards smearing at a higher molecular mass level. On the other hand, in the presence of Zn^{2+}, propofol caused remarkable upward band shifts from the single AQP4 tetramer in a dose-dependent manner (Figure 4A).

A correlation analysis revealed that there was a significant correlation between the reduced water permeability and the clustering of AQP4 tetramers caused by propofol in the presence of Zn^{2+} [$r = 0.794$ ($n = 18$); $P < 0.05$] (Figure 4B).

To validate the clustering effects of propofol and Zn^{2+} on AQP4 tetramers observed in BN-PAGE, we additionally performed a sucrose-density-gradient fractionation for AQP4 proteoliposomes treated with propofol and $ZnCl_2$ (Supplementary Figure S3 at http://www.biochemj.org/bj/454/bj4540275add.htm). The peak immunoreactivity was apparently shifted to the higher-density fraction in AQP4 proteoliposomes treated with propofol and $ZnCl_2$, further supporting the clustering effects of propofol with Zn^{2+}.

Inhibitory effects of propofol and Zn^{2+} on AQP4 proteoliposomes are reversible

Next, we examined the reversibility of the propofol-induced inhibition of AQP4. The above findings clearly indicated that the presence of Zn^{2+} is a pre-requisite for propofol-induced inhibition. Thus we asked whether the propofol-induced inhibition of AQP4 proteoliposomes could be reversed through the

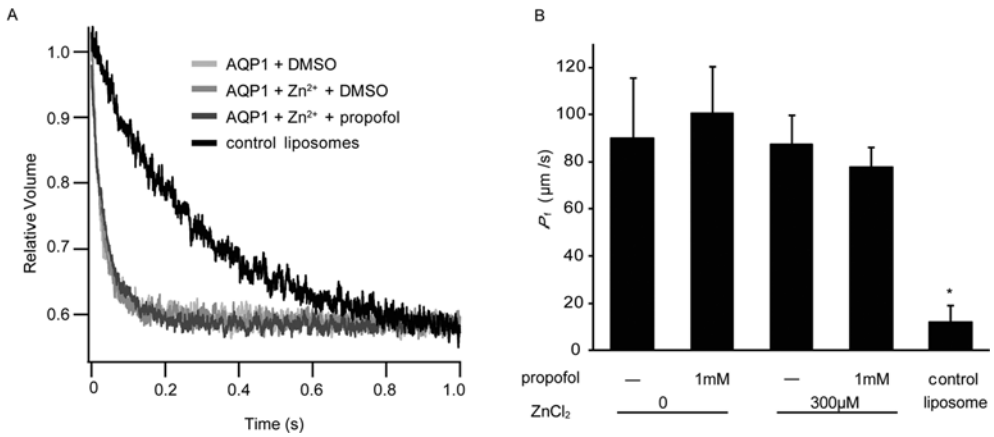

Figure 2 Propofol inhibition cannot be observed in AQP1 proteoliposomes

(**A**) Representative time courses for the hyperosmotic shrinkage of AQP1 proteoliposomes incubated with 0.1 % DMSO; 300 μM $ZnCl_2$ for 5 min, followed by 0.1 % DMSO for 15 min; or 300 μM $ZnCl_2$ for 5 min, followed by 1 mM propofol for 15 min as indicated; results for control liposomes are also shown (black). (**B**) The P_f of AQP1 proteoliposomes treated with $ZnCl_2$ and propofol. AQP1 proteoliposomes were treated as indicated and the P_f measurements were performed as described in Figure 1. The results are shown as the means $\pm$ S.D. ($n = 3$). *$P < 0.05$, compared with no-treatment group as analysed using a Student's unpaired *t* test.

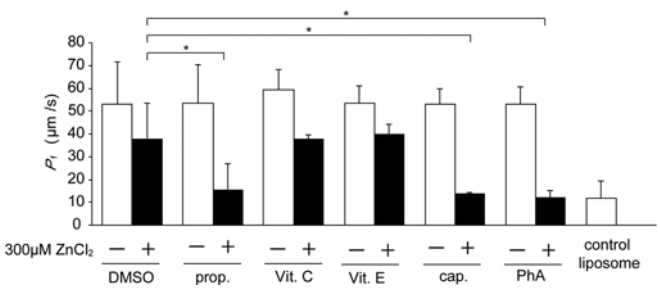

Figure 3 Effects of antioxidants or lipid membrane fluidizers on the P_f of AQP4 proteoliposomes in the presence of Zn^{2+}

AQP4 proteoliposomes were incubated with 300 μM $ZnCl_2$ for 5 min, followed by treatment with 1 mM propofol (prop.), lipophilic antioxidants [1 mM ascorbyl palmitate (Vit. C) and 1 mM α-tocopherol (Vit. E)] or lipid membrane fluidizers [1 mM capsaicin (cap.) and 20 mM phenethyl alcohol (PhA)] for 15 min at room temperature (22 °C), and the P_f was measured as described in Figure 1. The results are shown as the means $\pm$ S.D. ($n = 3$–5). *$P < 0.05$, as analysed using a Student's unpaired *t* test.

removal of Zn^{2+} using EDTA treatment. In line with a previous report [13], the inhibitory effect of Zn^{2+} alone was almost totally abolished by EDTA treatment [$P_f = 40.8 \pm 14.7$ μm/s compared with $P_f = 74.4 \pm 28.9$ μm/s ($n = 5$) respectively; $P < 0.05$] (Figure 5B). In addition, albeit not complete, the profound inhibition caused by propofol was remarkably reversed by the removal of Zn^{2+} [$P_f = 26.8 \pm 4.8$ μm/s compared with $P_f = 56.4 \pm 15.7$ μm/s ($n = 4$) respectively; $P < 0.05$] (Figures 5A and 5B). In agreement with this functional reversibility, the band shifts caused by propofol and Zn^{2+} observed in BN-PAGE was also apparently reversed by the removal of Zn^{2+} with EDTA treatment (Figure 5C). These findings indicate that the functional modulation caused by propofol and Zn^{2+} is, at least to some extent, reversible, and AQP4 is able to regain its function after the removal of Zn^{2+}.

Thiol modification of Cys^{253} by Zn^{2+} is essential for propofol inhibition

Given the high affinity of Zn^{2+} to cysteine residues in proteins, we tentatively examined whether propofol inhibition could be altered when reactivity of cysteine residues was masked by NMM (*N*-methylmaleimide), a thiol-covalent-modifying reagent (Figure 6A). Pre-treatment with NMM attenuated the inhibitory effect of Zn^{2+} alone. Moreover, in NMM-pre-treated AQP4 proteoliposomes, propofol rather enhanced the P_f of AQP4 both in the presence and absence of Zn^{2+} (Figure 6B). These findings suggest that thiol modification of cysteine residues by Zn^{2+} has an important role in propofol inhibition.

Next, we performed the site-directed mutagenesis experiments to determine which cysteine residue was responsible for the interaction with Zn^{2+} in propofol inhibition. Among six cysteine residues in AQP4 M23 isoform, we focused on two cysteine residues, Cys^{178} and Cys^{253}, which reportedly have important roles in metal inhibitions [12,13]. As expected, the inhibitory effect of Zn^{2+} alone was abolished in C178S-mutant AQP4 proteoliposomes in which Cys^{178} was mutated to a serine residue. However, the combination of propofol and Zn^{2+} continued to inhibit the C178S-mutant AQP4 proteoliposomes [45.7 $\pm$ 14.7 % inhibition ($n = 4$) respectively; $P < 0.05$] (Figure 7A, left-hand panel). In sharp contrast, propofol inhibition was remarkably attenuated in C253S-mutant AQP4 proteoliposomes in which Cys^{253} was replaced by a serine residue [13.1 $\pm$ 18.4 % inhibition ($n = 3$) respectively] (Figure 7A, middle panel). This suggests that the interaction between Zn^{2+} and Cys^{253} has an essential role in propofol inhibition on AQP4. Eventually, the inhibitory effects of propofol and Zn^{2+} were totally abolished in C178S/C253S double mutant AQP4 proteoliposomes (Figure 7A, right-hand panel). Consistent with these functional analyses, no clustering effect was observed in C178S/C253S double mutant AQP4 proteoliposomes (Figure 7B).

DISCUSSION

In the present study, we have discovered that propofol reversibly and specifically inhibits AQP4 in the presence of Zn^{2+} using an AQP4 proteoliposome functional assay. To our knowledge, the present study is the first to demonstrate that the water permeability of AQP4 can be affected by propofol, although propofol has been reported to influence the expression levels of AQP4 in cultured cells [28,29]. In addition, we identified Cys^{253} as a key residue for propofol inhibition. Since little attention has been paid to this residue with respect to the functional modulation of AQP4, our findings may provide novel insights into the functional regulation of AQP4.

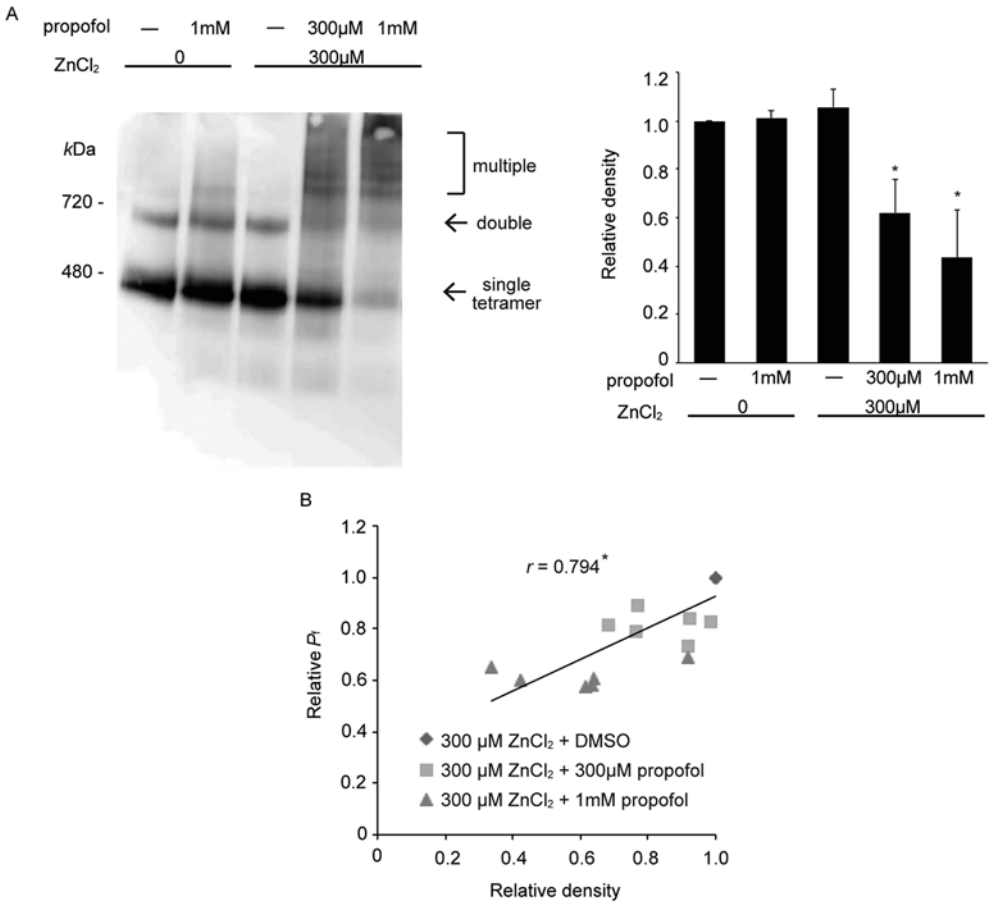

Figure 4 Propofol facilitates the clustering of AQP4 proteins in the presence of Zn^{2+}

(**A**) A representative result of BN-PAGE immunoblots for AQP4 M23 proteoliposomes treated with $ZnCl_2$ and propofol (left-hand panel). AQP4 proteoliposomes were treated with 300 μM $ZnCl_2$ for 5 min, followed by additional treatment with the indicated concentrations of propofol for 15 min at room temperature (22 °C). Then, the proteoliposomes were solubilized in 1 % *n*-dodecyl-β-D-maltoside, and BN-PAGE immunoblotting was performed. The clustering of AQP4 tetramers by the combination of $ZnCl_2$ and propofol was assessed by densitometry of the BN-PAGE immunoblots (right-hand panel). The band density corresponding to the single tetramer of no-treatment AQP4 proteoliposomes was assigned as the control and the relative densities of the single tetramer bands of AQP4 proteoliposomes treated with $ZnCl_2$ and propofol as indicated are displayed. The results are shown as means $\pm$ S.D. ($n = 3$). $^*P < 0.05$, compared with no-treatment group as analysed using a Student's unpaired *t* test. (**B**) The correlation between the reduced water permeability and the clustering of AQP4 tetramers caused by $ZnCl_2$ and propofol. The P_f and the BN-PAGE band density corresponding to the single tetramer of AQP4 proteoliposomes treated with 300 μM $ZnCl_2$ alone were assigned as controls and relative P_f of AQP4 proteoliposomes treated with 300 μM and 1 mM propofol were plotted as a function of relative density of the AQP4 single tetramer band. Pearson's correlation coefficient (*r*) was calculated using PASW Statistics 18.0 (SPSS) and displayed ($n = 18$; $^*P < 0.05$).

In a proteoliposome assay system we used, the proteins are supposed to be randomly incorporated in the lipid membrane in two orientations [12]. This property allows the externally applied Zn^{2+} to interact with cytoplasmic residues including Cys^{178} and Cys^{253}. However, the inhibitory effects caused by the combination of Zn^{2+} and propofol exceeded 50 % inhibition. As discussed in the previous report, one possibility is that some fraction of heavy metal ion could permeate through the lipid membrane and thereby affects the cysteine residues of AQP4 in both orientations [12]. It is also possible that a larger population of AQP4 proteins could be incorporated in one orientation, in which the cytoplasmic side is exposed to the outside of the vesicle. In fact, AQP4 proteins reconstituted in *E. coli* membrane showed a strong preference in their orientation shown by the structural analysis [30].

In contrast to AQP4, incubation with propofol either in the presence or absence of Zn^{2+} failed to significantly inhibit AQP1, despite its considerable structural and functional similarity to AQP4. Thus propofol-induced inhibition is, at least to some degree, specific to AQP4. A lack of the cysteine residue in AQP1 corresponding to Cys^{253} of AQP4 may concur with the specificity of propofol inhibition for AQP4, which is indicated by the site-directed mutagenesis. This specificity may be of great importance, especially for the development of AQP4-specific inhibitors.

It was noted that the presence of Zn^{2+} is required for the inhibition of AQP4 by propofol. The site-directed mutagenesis study revealed that the interaction between Zn^{2+} and Cys^{253} has an essential role in propofol inhibition. One possible underlying mechanism for this inhibition is a direct interaction among propofol, Zn^{2+} and Cys^{253}, which may cause a conformational change at a single channel level, leading to an interference with the water permeation through the pore. Since Cys^{253} is located at the membrane interface in the sixth transmembrane domain connecting to the C-terminal tail, the region including Cys^{253} is expected to be highly mobile. Thus the modulation of this residue may lead to a great structural change. Another possibility is that Zn^{2+} may mediate a tetramer–tetramer interaction through interacting with Cys^{253} residues of adjacent tetramers and thereby cause allosteric functional modulation. This type of Zn^{2+}-mediated clustering has been proposed in other proteins [31–33]. Since Cys^{253} is positioned at the outside surface of the AQP4 tetramer,

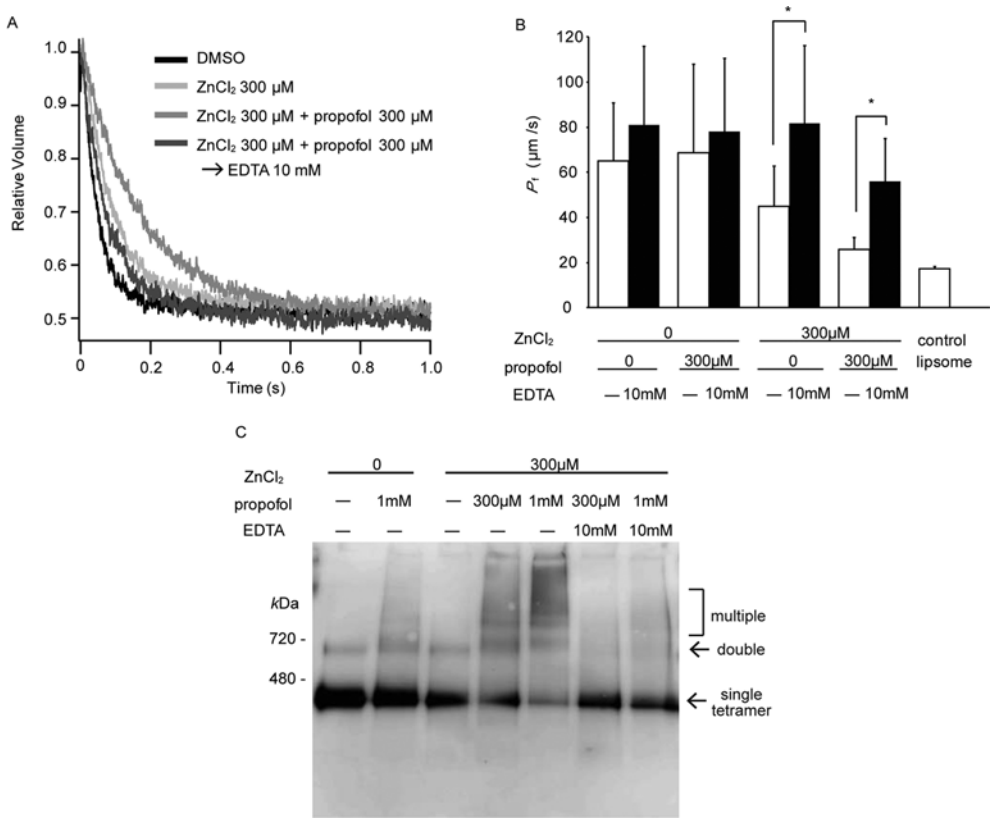

Figure 5 Reversibility of the effects of $ZnCl_2$ and propofol on AQP4 proteoliposomes

AQP4 proteoliposomes incubated with 300 μM $ZnCl_2$ and 300 μM propofol were treated with 10 mM EDTA for 10 min at room temperature (22 °C) and washed using ultracentrifugation. (**A**) Representative time courses for the hyperosmotic shrinkage of AQP4 proteoliposomes incubated with 0.1 % DMSO; 300 μM $ZnCl_2$, followed by 0.1 % DMSO; 300 μM $ZnCl_2$, followed by 300 μM propofol; or 300 μM $ZnCl_2$, followed by 300 μM propofol and treatment with 10 mM EDTA as indicated. (**B**) The P_f of AQP4 proteoliposomes treated with $ZnCl_2$ and propofol without (white) or with EDTA treatment (black). The measurements were performed as described in Figure 1. The results are shown as the means ± S.D. ($n = 3$). *$P < 0.05$, as analysed using a Student's unpaired t test. (**C**) The clustering of AQP4 proteins caused by Zn^{2+} and propofol was also reversible. AQP4 proteoliposomes incubated with $ZnCl_2$ and propofol with or without EDTA treatment were subjected to BN-PAGE immunoblotting, as described in Figure 4.

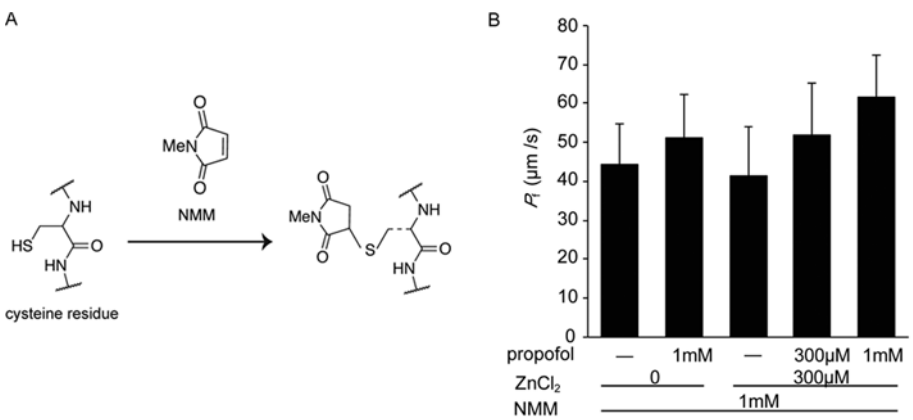

Figure 6 Cysteine-modification reagent NMM completely abolishes the propofol inhibition on the P_f of AQP4 proteoliposomes

(**A**) A chemical model of cysteine modification by NMM. (**B**) The P_f of AQP4 proteoliposomes treated with $ZnCl_2$ and propofol in the presence of NMM. AQP4 proteoliposomes incubated with 1 mM NMM for 10 min were treated with $ZnCl_2$ and propofol as indicated and the P_f values were measured as described in Figure 1. The results are shown as the means ± S.D. ($n = 3$).

it would be possible that Zn^{2+} may form co-ordination bonds with Cys^{253} residues of neighbouring AQP4 tetramers. Indeed, our BN-PAGE analysis has demonstrated the Zn^{2+}–Cys^{253}-dependent clustering of AQP4 in propofol inhibition, which is correlated with the reduced water permeability. Propofol may function to provide an environment for Zn^{2+} to mediate AQP4 cluster formation, plausibly through lipid membrane fluidization, since propofol has been shown to increase lipid membrane fluidity by penetrating superficially into the lipid bilayer and to facilitate the lateral diffusion of constituents in the lipid membrane [18,34]. The lateral mobility of AQP4 on the lipid membrane is also affected by temperature [35], suggesting that the behaviour of

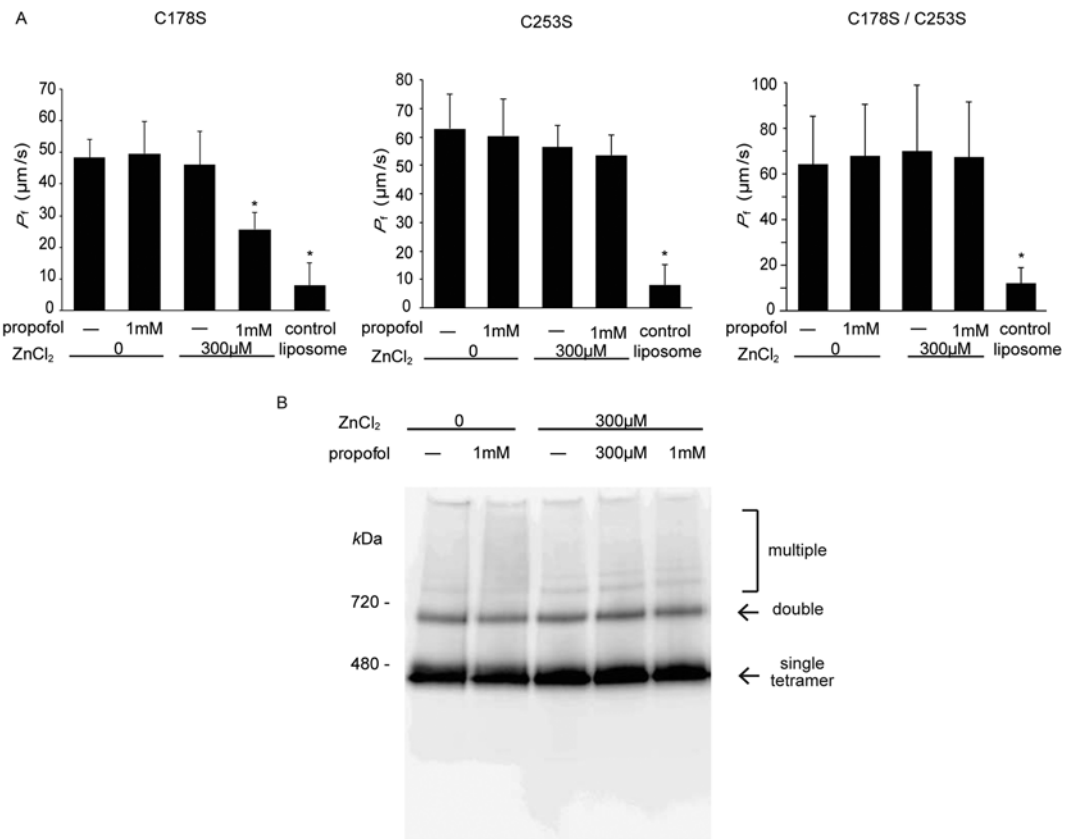

Figure 7 Roles of thiol modification of reactive cysteine residues in the inhibition of AQP4 caused by $ZnCl_2$ and propofol

(**A**) The P_f of mutant AQP4 (left-hand panel, C178S; middle panel, C253S; right-hand panel, C178S/C253S) proteoliposomes treated with $ZnCl_2$ and propofol as indicated. The results are shown as the means ± S.D. ($n = 3$–5). *$P < 0.05$, compared with no-treatment group as analysed using a Student's unpaired t test. (**B**) A representative result of BN-PAGE immunoblottings of C178S/C253S double mutant AQP4 proteoliposomes treated with $ZnCl_2$ and propofol as indicated.

AQP4 tetramers in the lipid membrane can be governed by protein–lipid interaction. Therefore it is possible that propofol-induced membrane fluidization might contribute to the Zn^{2+}-mediated AQP4 clustering and the functional inhibition, although specific interactions between propofol and AQP4 cannot be totally excluded. The inhibitory effects of other lipid membrane fluidizers observed in the present study may further support this possibility.

AQP4 is also known to form physiologically large clusters called OAPs (orthogonal arrays of particles) [36,37], which is reportedly mediated by the interactions among N-terminal chains and related to water permeation through AQP4 [23,38–40]. However, propofol inhibition of AQP4 is not directly related to the OAP formation since propofol inhibition is also observed in AQP4 M1 that is a shorter splicing isoform not capable of forming OAPs. Hence Zn^{2+}-mediated AQP4 clustering may involve a different mechanism from the physiological OAP formation and thereby affect the water permeability of AQP4 differently. Although the induction of AQP4 clustering by propofol and Zn^{2+} could be caused by proteotoxicity arising from the aggregation and denaturation of the protein, we believe that this is not the case because both the functional inhibition and the clustering are reversed after Zn^{2+} removal by the addition of EDTA. Nevertheless, more extensive structural analyses are required to determine how Zn^{2+}-mediated clustering couples with the profound functional inhibition of AQP4. Such studies will also shed light on the involvement of tetramer–tetramer interactions in the functional regulation of AQP4.

The propofol concentrations required to inhibit AQP4 in the present study are considerably higher than the clinically relevant plasma concentration or those used in other *in vivo* experiments [41]. However, membrane-acting drugs like propofol should be preferentially incorporated and concentrated in membrane lipids in the brain. Indeed, in rabbits anaesthetized with propofol, the propofol concentration in the brain parenchyma is more than ten times higher than the plasma concentration after the intravenous infusion of propofol [42]. Considering that AQP4 is strongly localized to vascular end-feet of astrocyte surrounding the blood–brain barrier, it is no wonder that AQP4 could be exposed to such high concentrations of propofol in *in vivo* situations. Thus taking advantage of abundant free Zn^{2+} in astrocytes under pathological conditions, propofol might inhibit AQP4 and prevent the cytotoxic brain oedema. This possibility is consistent with previous reports in which propofol attenuates the brain oedema following ischaemic injury in mice models [19,20,43].

Overall, we have demonstrated that propofol reversibly and specifically inhibits the function of AQP4 through the interaction between Zn^{2+} and Cys^{253}. It is a subject of future investigations whether these inhibitory mechanisms can be applied to physiological settings. Nevertheless, our findings provide new insight into the functional regulation of AQP4 and the identification of novel AQP4-specific inhibitors.

AUTHOR CONTRIBUTION

Jungo Kato prepared the materials for the proteoliposomes, carried out the experiments, interpreted the data, assembled the figures and wrote the paper. Mariko Kato Hayashi designed the study and established the proteoliposome preparation. Shinnosuke Aizu prepared the materials for the proteoliposomes and carried out the experiments. Yoshinori

Yukutake established the conditions for the proteoliposome preparation, the stopped-flow measurement and BN-PAGE. Junzo Takeda designed the study and interpreted the data. Masato Yasui designed the study, interpreted the data for the entire study and wrote the paper.

FUNDING

This work was supported by Global Centers of Excellence Program for Human Metabolic System Biology of the Ministry of Education, Culture, Sports, Science and Technology Japan; Program for the Advancement of Next Generation Research Project of Keio University; and the Japan New Energy and Industrial Technology Development Organization (NEDO) [grant number P08005].

REFERENCES

1 Fishman, R. A. (1975) Brain edema. N. Engl. J. Med. **293**, 706–711
2 Nag, S., Manias, J. L. and Stewart, D. J. (2009) Pathology and new players in the pathogenesis of brain edema. Acta Neuropathol. **118**, 197–217
3 Kimelberg, H. K. (2005) Astrocytic swelling in cerebral ischemia as a possible cause of injury and target for therapy. Glia **50**, 389–397
4 Thrane, A. S., Rappold, P. M., Fujita, T., Torres, A., Bekar, L. K. and Takano, T. (2011) Signaling events elicited by cerebral edema. Proc. Natl. Acad. Sci. U.S.A. **108**, 846–851
5 Nase, G., Helm, P. J., Enger, R. and Ottersen, O. P. (2008) Water entry into astrocytes during brain edema formation. Glia **56**, 895–902
6 Nielsen, S., Nagelhus, E. A., Amiry-moghaddam, M., Bourque, C., Agre, P. and Ottersen, O. P. (1997) Specialized membrane domains for water transport in glial cells: high-resolution immunogold cytochemistry of aquaporin-4 in rat brain. J Neurosci. **17**, 171–180
7 Amiry-Moghaddam, M., Otsuka, T., Hurn, P. D., Traystman, R. J., Haug, F., Froehner, S. C., Adams, M. E., Neely, J. D., Agre, P., Ottersen, O. P. and Bhardwaj, A. (2002) An α-syntrophin-dependent pool of AQP4 in astroglial end-feet confers bidirectional water flow between blood and brain. Proc. Natl. Acad. Sci. U.S.A. **100**, 2106–2111
8 Papadopoulos, M. C. and Verkman, A. S. (2007) Aquaporin-4 and brain edema. Pediatr. Nephrol. **22**, 778–784
9 Verkman, A. S., Binder, D. K., Bloch, O., Auguste, K. and Papadopoulos, M. C. (2006) Three distinct roles of aquaporin-4 in brain function revealed by knockout mice. Biochim. Biophys. Acta **1758**, 1085–1093
10 Manley, G. T., Fujimura, M., Ma, T., Noshita, N., Filiz, F., Bollen, A. W., Chan, P. and Verkman, A. S. (2000) Aquaporin-4 deletion in mice reduces brain edema after acute water intoxication and ischemic stroke. Nat. Med. **6**, 159–163
11 Papadopoulos, M. C. and Verkman, A. S. (2005) Aquaporin-4 gene disruption in mice reduces brain swelling and mortality in pneumococcal meningitis. J. Biol. Chem. **280**, 13906–13912
12 Yukutake, Y., Tsuji, S., Hirano, Y., Adachi, T., Takahashi, T., Fujihara, K., Agre, P., Yasui, M. and Suematsu, M. (2008) Mercury chloride decreases the water permeability of biology of aquaporin-4-reconstituted proteoliposomes. Biol. Cell **100**, 355–363
13 Yukutake, Y., Hirano, Y., Suematsu, M. and Yasui, M. (2009) Rapid and reversible inhibition of aquaporin-4 by zinc. Biochemistry **48**, 12059–12061
14 Kruczek, C., Görg, B., Keitel, V., Pirev, E., Kröncke, K. D., Schliess, F. and Häussinger, D. (2009) Hypoosmotic swelling affects zinc homeostasis in cultured rat astrocytes. Glia **57**, 79–92
15 Franks, N. P. (2008) General anaesthesia: from molecular targets to neuronal pathways of sleep and arousal. Nat. Rev. Neurosci. **9**, 370–386
16 Trapani, G., Altomare, C., Sanna, E. and Liso, G. (2000) Propofol in anesthesia. Mechanism of action, structure–activity relationships, and drug delivery. Curr. Med. Chem. **7**, 249–271
17 Balasubramanian, S. V, Campbell, R. B. and Straubinger, R. M. (2002) Propofol, a general anesthetic, promotes the formation of fluid phase domains in model membranes. Chem. Phys. Lipids **114**, 35–44
18 Tsuchiya, H. (2001) Structure-specific membrane fluidizing effect of propofol. Clin. Exp. Pharmacol. Physiol. **28**, 292–299
19 Adembri, C., Venturi, L., Tani, A., Chiarugi, A., Gramigni, E., Cozzi, A., Pancani, T., De Gaudio, R. A. and Pellegrini-Giampietro, D. E. (2006) Neuroprotective effects of propofol in models of cerebral ischemia: inhibition of mitochondrial swelling as a possible mechanism. Anesthesiology **104**, 80–89
20 Kotani, Y., Nakajima, Y., Hasegawa, T., Satoh, M., Nagase, H., Shimazawa, M., Yoshimura, S., Iwama, T. and Hara, H. (2008) Propofol exerts greater neuroprotection with disodium edetate than without it. J. Cereb. Blood Flow Metab. **28**, 354–366
21 Yang, B., Van Hoek, A. N. and Verkman, A. S. (1997) Very high single channel water permeability of aquaporin-4 in baculovirus-infected insect cells and liposomes reconstituted with purified aquaporin-4. Biochemistry **36**, 7625–7632
22 Zeidel, M. L., Albalak, A., Grossman, E. and Carrutherss, A. (1992) Role of glucose carrier in human erythrocyte water permeability. Biochemistry **31**, 589–596
23 Crane, J. M. and Verkman, A. S. (2009) Determinants of aquaporin-4 assembly in orthogonal arrays revealed by live-cell single-molecule fluorescence imaging. J. Cell Sci. **122**, 813–821
24 Aarts, L., Van der Hee, R., Dekker, I., Jong, J., de Langemeijer, H. and Bast, A. (1995) The widely used anesthetic agent propofol can replace as an antioxidant-tocopherol. FEBS Lett. **357**, 83–85
25 Vasileiou, I., Xanthos, T., Koudouna, E., Perrea, D., Klonaris, C., Katsargyris, A. and Papadimitriou, L. (2009) Propofol: a review of its non-anaesthetic effects. Eur. J. Pharmacol. **605**, 1–8
26 Sorbo, J. G., Moe, S. E., Ottersen, O. P. and Holen, T. (2008) The molecular composition of square arrays. Biochemistry **48**, 2631–2637
27 Nicchia, G. P., Rossi, A., Mola, M. G., Pisani, F., Stigliano, C., Basco, D., Mastrototaro, M., Svelto, M. and Frigeri, A. (2010) Higher order structure of aquaporin-4. Neuroscience **168**, 903–914
28 Zheng, Y. Y., Lan, Y. P., Tang, H. F. and Zhu, S. M. (2008) Propofol pretreatment attenuates aquaporin-4 over-expression and alleviates cerebral edema after transient focal brain ischemia reperfusion in rats. Anesth. Analg. **107**, 2009–2016
29 Zhu, S. M., Xiong, X. X., Zheng, Y. Y. and Pan, C. F. (2009) Propofol inhibits aquaporin 4 expression through a protein kinase C-dependent pathway in an astrocyte model of cerebral ischemia/reoxygenation. Anesth. Analg. **109**, 1493–1499
30 Hiroaki, Y., Tani, K., Kamegawa, A., Gyobu, N., Nishikawa, K., Suzuki, H., Walz, T., Sasaki, S., Mitsuoka, K., Kimura, K. et al. (2006) Implications of the aquaporin-4 structure on array formation and cell adhesion. J. Mol. Biol. **355**, 628–639
31 Maret, W. and Li, Y. (2009) Coordination dynamics of zinc in proteins. Chem. Rev. **109**, 4682–4707
32 Gundelfinger, E. D., Boeckers, T. M., Baron, M. K. and Bowie, J. U. (2006) A role for zinc in postsynaptic density assembly and plasticity. Trends Biochem. Sci. **31**, 366–373
33 Conrady, D. G., Brescia, C. C., Horii, K., Weiss, A. A., Hassett, D. J. and Herr, A. B. (2008) A zinc-dependent adhesion module is responsible for intercellular adhesion in staphylococcal biofilms. Proc. Natl. Acad. Sci. U.S.A. **105**, 19456–19461
34 Momo, F., Fabris, S., Bindoli, A., Scutari, G. and Stevanato, R. (2002) Different effects of propofol and nitrosopropofol on DMPC multilamellar liposomes. Biophys. Chem. **95**, 145–155
35 Crane, J. M. and Verkman, A. S. (2009) Reversible, temperature-dependent supramolecular assembly of aquaporin-4 orthogonal arrays in live cell membranes. Biophys. J. **97**, 3010–3018
36 Furman, C. S., Gorelick-Feldman, D. A., Davidson, K. G. V, Yasumura, T., Neely, J. D., Agre, P. and Rash, J. E. (2003) Aquaporin-4 square array assembly: opposing actions of M1 and M23 isoforms. Proc. Natl. Acad. Sci. U.S.A. **100**, 13609–13614
37 Rash, J. E., Davidson, K. G. V., Yasumura, T. and Furman, C. S. (2004) Freeze-fracture and immunogold analysis of aquaporin-4 (AQP4) square arrays, with models of AQP4 lattice assembly. Neuroscience **129**, 915–934
38 Fenton, R. A, Moeller, H. B., Zelenina, M., Snaebjornsson, M. T., Holen, T. and MacAulay, N. (2010) Differential water permeability and regulation of three aquaporin 4 isoforms. Cell. Mol. Life Sci. **67**, 829–840
39 Neely, J. D., Christensen, B. M., Nielsen, S. and Agre, P. (1999) Heterotetrameric composition of aquaporin-4 water channels. Biochemistry **38**, 11156–11163
40 Silberstein, C., Bouley, R., Huang, Y., Fang, P., Pastor-Soler, N., Brown, D. and Van Hoek, A. N. (2004) Membrane organization and function of M1 and M23 isoforms of aquaporin-4 in epithelial cells. Am. J. Physiol. Renal Physiol. **287**, F501–F511
41 Shafer, A., Doze, VA. and Shafer, S. W. P. (1988) Pharmacokinetics and pharmacodynamics of propofol infusions during general anesthesia. Anesthesiology **69**, 348–356
42 Riu, P. L., Riu, G., Testa, C., Mulas, M., Caria, M. A., Mameli, S. and Mameli, O. (2000) Disposition of propofol between red blood cells, plasma, brain and cerebrospinal fluid in rabbits. Eur. J. Anaesthesiol. **17**, 18–22
43 Wang, J., Yang, X., Camporesi, C. V, Yang, Z., Bosco, G., Chen, C. and Camporesi, E. M. (2002) Propofol reduces infarct size and striatal dopamine accumulation following transient middle cerebral artery occlusion: a microdialysis study. Eur. J. Pharmacol. **452**, 303–308

Received 8 January 2013/22 May 2013; accepted 17 June 2013
Published as BJ Immediate Publication 17 June 2013, doi:10.1042/BJ20130046

Biochem. J. (2013) **454**, 275–282 (Printed in Great Britain) doi:10.1042/BJ20130046

online data

SUPPLEMENTARY ONLINE DATA

A general anaesthetic propofol inhibits aquaporin-4 in the presence of Zn^{2+}

Jungo KATO*†, Mariko Kato HAYASHI†, Shinnosuke AIZU†, Yoshinori YUKUTAKE‡, Junzo TAKEDA* and Masato YASUI†[1]

*Department of Anesthesiology, School of Medicine, Keio University, Tokyo 160–8582, Japan, †Department of Pharmacology, School of Medicine, Keio University, Tokyo 160–8582, Japan, and ‡Department of Biochemistry, School of Medicine, Keio University, Tokyo 160–8582, Japan

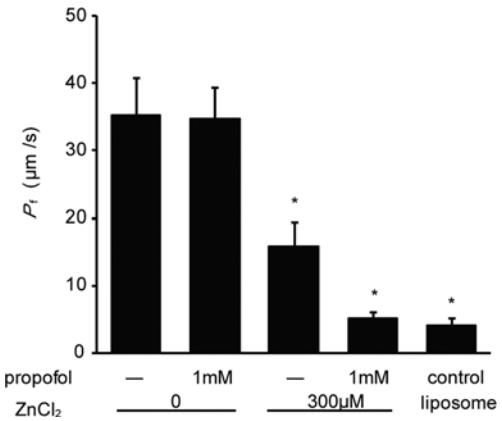

Figure S1 Effects of propofol and Zn^{2+} on AQP4 proteoliposomes without the His-tag

The inhibitory effects of $ZnCl_2$ and propofol on AQP4 were not due to an artefact caused by the His-tag at the N-terminal of the purified AQP4 protein. The P_f of His-tag (−) AQP4 proteoliposomes were treated with $ZnCl_2$ and propofol. AQP4 proteins in which the His-tags at the N-terminal were cleaved were reconstituted into liposomes. The treatments and measurements were performed as described in Figure 1 in the main text. The results are shown as the means ± S.D. ($n = 3$). *$P < 0.05$, as analysed using a Student's unpaired t test.

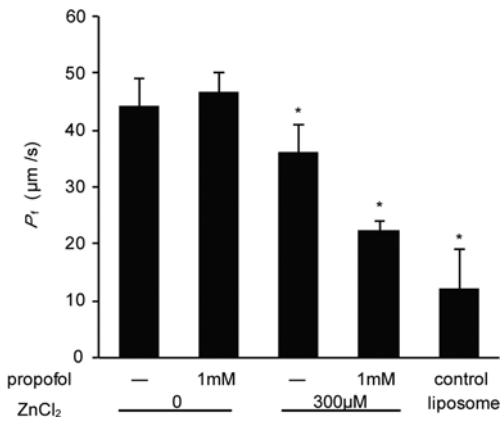

Figure S2 Combination effects of $ZnCl_2$ and propofol were also observed in AQP4 M1 proteoliposomes

P_f of AQP4 M1 proteoliposomes treated with $ZnCl_2$ and propofol. The treatments and measurements were performed as described in Figure 1 in the main text. The results are shown as the means ± S.D. ($n = 3$). *$P < 0.05$, as analysed using a Student's unpaired t test.

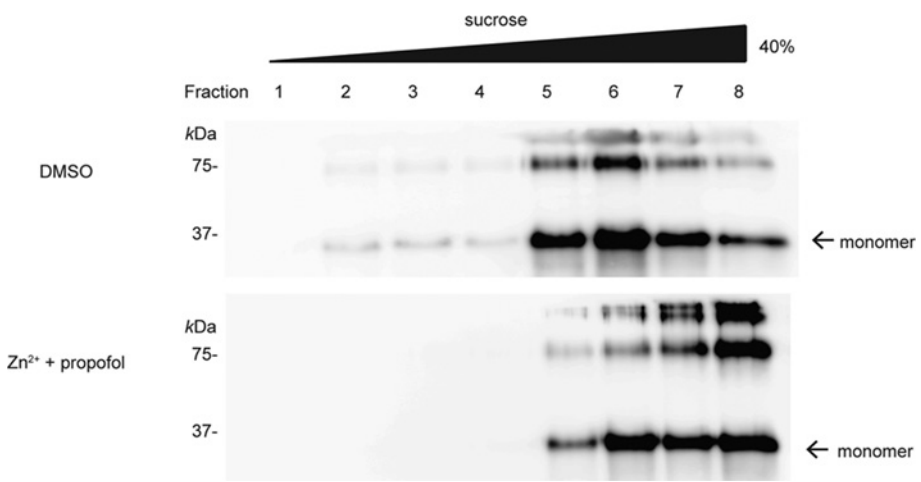

Figure S3 Sucrose-density-gradient fractionation for AQP4 proteoliposomes treated with $ZnCl_2$ and propofol

AQP4 proteoliposomes treated with DMSO or the combination of 300 μM $ZnCl_2$ and 1 mM propofol were solubilized with 1 % n-dodecyl-β-D-maltoside and subjected to sucrose-gradient-density centrifugation. Aliquots collected from top to bottom were subjected to SDS/PAGE (12 % gel) and immunoblotted for AQP4.

Received 8 January 2013/22 May 2013; accepted 17 June 2013
Published as BJ Immediate Publication 17 June 2013, doi:10.1042/BJ20130046

[1] To whom correspondence should be addressed (email myasui@a3.keio.jp).